Electronic Letters on Computer Vision and Image Analysis 22(2):41-52, 2023

Robust fingerprint recognition approach based on diagonal slice of polyspectra in the polar space

E.M ISMAILI ALAOUI

Faculty of Sciences, Moulay Ismail University, Meknes-Morocco

Received 9th of October, 2021; accepted 19th of December 2023

Abstract

Although fingerprint recognition is a mature technology and nowadays commercial state-of-the-art systems can be successfully used in a number of real applications, not all the problems have been solved and the research is still very active in the field. This paper presents a new approach for estimating the shift and rotation parameters between fingerprint images stored in the database that operates in the third-order frequency-domain measure called the auto-bispectrum, which, allows us to estimate the shift and the rotation separately. The diagonal slices and their spectra of auto- and cross-bispectrum are proposed. The rotation parameters are estimated from the remaining polar sampled the third-order spectrum using cross-correlation, and then, after compensating for rotation, we may easily estimate the translational component, e.g., by using phase correlation. Experimental evidence of this performance is presented, and the mathematical reasons behind these characteristics are explained in depth. We compare our approach in a simulation to other frequency-domain fingerprint recognition algorithms. We find that our algorithm can better estimate shift and rotation parameters than the other methods.

Key Words: Biometric, Fingerprint Matching, Fingerprint Recognition, Auto-Bispectrum, Cross-Bispectrum, Diagonal Slices, Shift-Rotation Fingerprint, Polar Space ,Rotation Estimation, Sub-Pixel Shift Estimation.

1 Introduction

Individual recognition systems with high-speed and high-accuracy have been recently demanded in the automatic logging into a PC, the immigration at the airport, the access control and diligence and indolence management in an office, and so on. Biometric authentication is now being regarded as the most valid method because of the receptivity, individuality and invariability of biometric identifiers. Various types of the individual recognition systems based on biometrics have been studied and partially realized. Fingerprints, faces, hand geometry, irises, vein patterns, gait, signatures, etc., are known as biometric identifiers. Among the many biometric traits, the fingerprint is considered one of the most studied biometric traits and the most widely used in civil and forensic applications. Fingerprints are easily accessible, recognition requires minimal effort on the part of the user, it does not capture information other than strictly necessary for the recognition process, and provides relatively good performance. Another reason for the popularity of fingerprints is the individuality,

Correspondence to: e.ismailialaoui@fs.umi.ac.ma

Recommended for acceptance by Angel D. Sappa
https://doi.org/10.5565/rev/elcvia.1523
ELCVIA ISSN:1577-5097
Published by Computer Vision Center / Universitat Autonoma de Barcelona, Barcelona, Spain

persistence, relatively low cost and maturity of the existing products.
PC keyboards and smart cards with built-in fingerprint sensors are already available on the market, and the sensors can be integrated easily in wireless hardware [1, 2].
While law enforcement agencies were the earliest adopters of the fingerprint recognition technology, increasing concerns about national security, financial fraud and identity fraud have determined a growing need for this technology for person recognition in a number of non-forensic applications.
Even if fingerprints were first introduced as a method for person identification over 100 years ago and nowadays all forensics and law enforcement agency world-wide uses automatic fingerprint identification systems, fingerprint recognition cannot be considered a fully solved problem. On the contrary, it is still a challenging and important pattern recognition problem because of the large intraclass variability and large inter-class similarity in fingerprint patterns. The main causes of intra-class variations are: i) displacement, ii) rotation, iii) partial overlap, iv) non-linear distortion, v) variable pressure, vi) skin distortion, vii) noise, and viii) feature extraction errors. Therefore, fingerprints from the same finger may sometimes look quite different, while fingerprints from different fingers may appear quite similar.
The problem of fingerprint matching has been extensively studied and numerous algorithms have been proposed. These algorithms can be classified as correlation-based [3, 4, 5, 6, 7, 9, 8, 10, 11, 12, 13, 14, 15], minutiae-based [17, 18, 19, 20] and frequency-based [21, 22] approaches. Correlation-based matching is the most popular and widely used technique, being the basis of the fingerprint comparison.

2 Previous work and motivation

In the literature a number of correlation based algorithms may be found. Among the most important aspects of these techniques are the selection of appropriate areas of the fingerprint image for correlation and the computational effort required to consider translation and rotation between the fingerprint images. An efficient correlation-based method is the phase-based method [3]. A phase-only correlation (POC) method was first proposed in [4]. This method adopted the Fourier phase information and changed fingerprint images from the spatial-domain to the frequency-domain. Bazen et al. [5] first choose appropriate templates from the primary fingerprint, then template matching are used to locate those templates on the input fingerprint, by comparing the positions of these templates one can decide if the two fingerprints match or not. This matching is based on the correlation scores from the intensities of corresponding pixels of template and input fingerprint. Jain et al. [6] developed a hybrid matching algorithm that uses both minutiae information and texture information for matching the fingerprints. Nandkumar et al. [7] proposed a local correlation based fingerprint matching algorithm. The normalized cross-correlation between the query window and template window is computed and peak is detected. The local correlation of all template windows with the corresponding regions in the query image are computed and mean correlation value is found. In this way all the possible correspondence from the alignment stage are tested and maximum correlation value over all the correspondence is taken as the matching score between the query and template image. In [15], a method of fingerprint recognition based on the DCT features of a discrete image is proposed. Its performance is evaluated by the k-nearest neighbor (k-NN) classifier. Ito et al. [9, 8] present a band limited phase only correlation (BLPOC) based image matching algorithm. BLPOC method is more robust to the noise and provides a sharper peak to distinguish between the genuine and imposter matching than POC method. In order to account for displacement and rotation, Ouyang et al. [10] describe a correlation based matching method using local Fourier-Mellin descriptor (FMD) and POC method. However, since the center of relative rotation between two compared fingerprints is unknown, the local FMD has to be extracted for a large number of center locations. There are some matching techniques been proposed under frequency-domain. Cavusoglu et al. [12] developed a robust correlation based fingerprint matching algorithm. The proposed algorithm requires segmentation, ridge orientation, reference point detection and normalized operation before the application of correlation algorithm.
In general, the correlation-based matching is not a robust method because the computational complexity is very expensive. This problem can improve efficiency by using FMT [11] that is based on the properties of the image

amplitude spectrum. Elena and Pavol also described a fingerprint verification method with the help of Fourier and FMT without broad preprocessing [14]. But, also the performance is degrades if the query and reference image contains much noise and that too of different types. Zaixing et al. [13] introduced a novel recognition algorithm using a limited ellipse-band-based matching method. It uses the FMT to improve the limitation of the original algorithm, which cannot resist rotation changes. Furthermore, an ellipse band on the frequency amplitude is used to suppress noise that is introduced by the high-frequency parts of images. In such circumstances, higher order statistics (HOS) in general and the auto-bispectrum in particular may offer more advantages since they are not affected by such noise [23].
Our main contribution in this paper consists of a new computationally efficient method based on HOS to estimate the motion parameters between fingerprint images. Although the basic idea of the method is quite similar to the 2D-FMT, it has certain advantages. The diagonal slices and their spectra of auto- and cross-bispectrum are proposed. Another important characteristic of our approach is that it avoids polar coordinates. In this way, it bypasses a numerically delicate step that represents both a potential threat for the original image information and a computationally intensive task. Rotation is isolated using the shift-rotation invariant properties of the cross-bispectrum of the two fingerprint images. Applying a polar transform to each magnitude spectrum converts rotation to be represented as translation, whereby phase correlation can be applied to recover the rotation angle between images. This enables us to estimate the change in orientation of image in a single calculation. Our matching algorithm is also known as diagonal slice of polyspectra in the polar space (DSP-PS). The motivation for using HOS, in particular auto-bispectrum comes from the following facts:

- Auto-bispectrum retains both amplitude and phase information from the Fourier coefficients of a signal, unlike ordinary second order power spectra and auto-correlation. The phase of the Fourier transform (FT) contains important shape information [24].
- Auto-bispectrum is shift-invariant because linear phase terms caused by translation are cancelled in the triple product of Fourier coefficients and it is also easier to generate features from auto-bispectrum that satisfy other desirable properties such as scaling, amplification, and rotation invariance [25].
- For one dimensional patterns, the Fourier phase is a shape-dependent nonlinear function of the frequency, and auto-bispectrum can extract this information [26].
- Multidimensional signals can be decomposed into one-dimensional projections. Transformations such as shift, scaling, or rotation of the multidimensional signal can be related to shift or scaling of the projections [26].
- Auto-bispectrum of Gaussian noise is identically zero, a fact which may be exploited to reduce additive noise effects, this provides high noise immunity to features. Further, the auto-bispectrum is immune to all the symmetrically distributed additive noise [25].
- When an image shifts and rotates, the auto-bispectrum merely rotates, whereas the Fourier spectrum alters in a more complicated fashion. The amplitude of the Fourier spectrum does exhibit the same rotation as the image [27].

3 Phase-based fingerprint matching

In order to study the effect of motion on the fingerprints FT, it is important to know how the spectrum is modified by the spatial changes associated with motion. Two particular features of the FT relating directly to motion estimation are its translational and rotational invariant properties [28].
Let $f(x, y)$ represent the registered fingerprint image, and $g(x, y)$ the input fingerprint image, which is but replica of $f(x, y)$ rotated by θ_0 and translated by (d_x, d_y), then we can write

$$g(x, y) = f(x\cos\theta_0 + y\sin\theta_0 - d_x, -x\sin\theta_0 + y\cos\theta_0 - d_y), \tag{1}$$

which, on FT, gives

$$G(u_x, u_y) = e^{-i2\pi(u_x d_x + u_y d_y)} F(u_x \cos\theta_0 + u_y \sin\theta_0, -u_x \sin\theta_0 + u_y \cos\theta_0), \tag{2}$$

where (u_x, u_y) is the frequency cordinates for the 2-D FT.
This comes from the Fourier rotation theorem that the 2-D FT rotates by the same angle as that of the object in the image space. We can rewrite the (2) as

$$G(u_x, u_y) = e^{-i2\pi(u_x d_x + u_y d_y)} F(u_x^{'}, u_y^{'}), \tag{3}$$

where $u_x^{'} = u_x \cos\theta_0 + u_y \sin\theta_0$ and $u_y^{'} - u_x \sin\theta_0 + u_y \cos\theta_0$.
$F(u_x^{'}, u_y^{'})$ is given by,

$$F(u_x^{'}, u_y^{'}) = \int_{-\infty}^{+\infty} \int_{-\infty}^{+\infty} f(x^{'}, y^{'}) e^{-i2\pi(u_x x^{'} + u_y y^{'})} dx^{'} dy^{'}, \tag{4}$$

where $x^{'} = \cos\theta_0 + y \sin\theta_0 - d_x$ and $y^{'} = -x \sin\theta_0 + y \cos\theta_0 - d_y$. $F(u_x^{'}, u_y^{'})$ can be written as a product of the phase and amplitude part of the image, $|F(u_x^{'}, u_y^{'})| e^{i\phi(u_x^{'}, u_y^{'})}$, where $|F(u_x^{'}, u_y^{'})|$ is the amplitude and $e^{i\phi(u_x^{'}, u_y^{'})}$ is the phase of the image. The phase part adds up with the translational phase $e^{-i2\pi(u_x x^{'} + u_y y^{'})}$. Extracting the amplitude part of the spectrum for shift-invariant processing erases the inherent phase information of the image.
Taking the modulus of both sides of (3), one sees that $|G(u_x, u_y)| = |F(u_x^{'}, u_y^{'})|$. This means that the rotational invariant property of the Fourier magnitude is preserved in this situation.
In summary, when there is both rotation and translation, the FT magnitude is preserved, but it is rotated.
There are at least three disadvantages related to the amplitude spectrum. Firstly, it does not provide a full description of the image contents, because it lacks the information carried by the phase spectrum. The amplitude spectrum is symmetric which means that the half of its values are redundant. As a consequence, half of the information is basically lost. Secondly, the amplitude spectrum is sensitive to illumination changes that is not a good basis for illumination invariant matching. Thirdly, it is necessary to perform pre-windowing before computing the amplitude spectrum in order to avoid the sinc effect in the resulting spectrum.
The motivation of using HOS comes not only from the properties of HOS but from a logical trajectory of recent developments of HOS in image processing.

4 Polyspectra correlation-based matching

4.1 HOS and auto-bispectrum

The widely applied conventional autocorrelation is a special case of a sequence of autocorrelations. A general $n-th$ order auto-cumulant of a stationary zero-mean 2-D random field $f(x, y)$ is defined as

$$C^{nf}(x_1, y_1; x_2, y_2; ...; x_{n-1}, y_{n-1}) = \int_{-\infty}^{+\infty} \int_{-\infty}^{+\infty} f(x, y) f(x + x_1, y + y_1) f(x + x_2, y + y_2) \\ ... f(x + x_{n-1}, y + y_{n-1}) dx dy \tag{5}$$

where (x, y) and (x_i, y_i) $(i = 1, 2, ..., n-1)$ are spatial position vectors. The FT of the $n-th$ order auto-cumulant is generally called the $n-th$ order spectrum. Spectra of order greater than 2 are termed HOS, which are also known as polyspectra. Among the polyspectra, the third-order spectrum, which is the FT of the third-order auto-cumulant or auto-triple correlation, is conventionally termed the auto-bispectrum.

As a compromise between accuracy of representation and computational complexity, we chose $n = 3$ in (5), the third-order auto-cumulant C^{fff} is given by

$$C^{fff}(x_1, y_1; x_2, y_2) = \int_{-\infty}^{+\infty} \int_{-\infty}^{+\infty} f(x, y) f(x + x_1, y + y_1) f(x + x_2, y + y_2) dx dy \tag{6}$$

The auto-bispectrum $B^{fff}(u_x, u_y; v_x, v_y)$ is related to the third-order auto-cumulant , $C^{fff}(x_1, y_1; x_2, y_2)$, by the well-known FT relationship [36]

$$B^{fff}(u_x, u_y; v_x, v_y) = \mathcal{F}^4[C^{fff}(x_1, y_1; x_2, y_2)] \tag{7}$$

where $\mathcal{F}^4$ denotes the 4-D Fourier transform operation, (u_x, u_y) and (v_x, v_y) are the frequency coordinates for the 2-D FT.
Each component of the auto-bispectrum is estimated by a triple product of Fourier coefficients as [36]

$$B^{fff}(u_x, u_y; v_x, v_y) = F(u_x, u_y) F(v_x, v_y) F^*(u_x + v_x, u_y + v_y) \tag{8}$$

where $*$ indicates the complex conjugate.
Actually, it can be the implement method in program and the computation load is evidently large. Hence, the diagonal slice was proposed to save the computational time.

4.2 Diagonal slice of auto-bispectrum

As we can see from (8) the auto-bispectrum has two vector arguments containing totally four scalar frequency variables. However, its costs much computer time, and the 2-D graph is very complex as compared with that of 1-D. Many scholars have done quite a number of researches in feature extraction and dimension reduction based on HOS. One of the outstanding works is the diagonal slice and its spectrum [30]. Diagonal slice of auto-bispectrum is a special condition on the $u_x = v_x$ and $u_y = v_y$ which not only can provide phase information but is much simpler and cost little computer time with a high-resolution ability in 1-D representation. The 1-D diagonal slice of auto-bispectrum can be given as:

$$B^{fff}(u_x, u_y; u_x, u_y) = B^{fff}(u_x, u_y) = F^2(u_x, u_y) F^*(2u_x, 2u_y) \tag{9}$$

As we can see from the equation, the computation load is cut down compared to auto-bispectrum.

5 Proposed fingerprint recognition approach

The auto- and cross-bispectrum consideration of motion has several advantages. There are two main reasons that may favor the frequency-domain HOS: robustness to noise and separability of the rotational and translational components. Indeed, the separability of rotation and translation is intrinsic in the structure of the Fourier representation of signals. Then a polar transformation is applied to the magnitude spectrum and the rotation is recovered by using phase correlation in the polar space. This method exploits the fact that by operating on the magnitude spectrum of an image, the translational differences are avoided since the magnitude spectrum of an image and its translated counterpart are identical; only their phase spectrum are different. Furthermore, the polar transformation causes rotation to be manifest as translation; we can then calculate the angle of rotation by cross correlation. Accordingly, we may first estimate the rotational component, and then, after compensating for rotation, we may easily estimate the translational component, e.g., by using phase correlation.
In subsection 5.1, we give a precise matching under rotation algorithm. A matching under sub-pixel shift algorithm is described in subsection 5.2.

5.1 Matching under rotation

One common method of determining the shift (d_x, d_y) and a planar rotation angle θ_0 is to compute the cross-bispectrum between $g(x, y)$ and $f(x, y)$. The latter is obtained in a similar manner as the auto-bispectrum. Thus,

$$B^{gfg}(u_x, u_y) = \mathcal{F}^4[C^{gfg}(x, y)] = G(u_x, u_y)F(u_x, u_y)G^*(2u_x, 2u_y) \tag{10}$$

Using the relation (3) we can transform (10) as:

$$B^{gfg}(u_x, u_y) = B^{fff}(u_x^{'}, u_y^{'})e^{-i2\pi(u_x d_x + u_y d_y)} \tag{11}$$

The relation between the amplitudes can be computed as

$$|B^{gfg}(u_x, u_y)| = |B^{fff}(u_x^{'}, u_y^{'})e^{-i2\pi(u_x d_x + u_y d_y)}| = |B^{fff}(u_x^{'}, u_y^{'})| \tag{12}$$

where $|B^{gfg}(u_x, u_y)|$ is a rotated version of $|B^{fff}(u_x, u_y)|$ over the same angle θ_0 as the spatial domain rotation. $|B^{fff}(u_x, u_y)|$ and $|B^{gfg}(u_x, u_y)|$ do not depend on the shift values (d_x, d_y), because the spatial domain shifts only affect the phase values of the $|B^{fff}(u_x, u_y)|$ and $|B^{gfg}(u_x, u_y)|$. Therefore we can first estimate the rotation angle θ_0 from the amplitudes of the $|B^{fff}(u_x, u_y)|$ and $|B^{gfg}(u_x, u_y)|$. After compensation for the rotation, the shift (d_x, d_y) can be computed from the phase difference between $B^{fff}(u_x, u_y)$ and $B^{gfg}(u_x, u_y)$. Let M^{gfg} and M^{fff} be the representations of $|B^{gfg}(u_x, u_y)|$ and $|B^{fff}(u_x, u_y)|$ in polar coordinates. So, we can rewrite (12) by

$$M^{gfg}(\rho, \theta) = M^{fff}(\rho, \theta - \theta_0) \tag{13}$$

where ρ and θ are the radius and angle in the polar coordinate system, respectively. $u_x = \rho\cos\theta$ and $u_y = \rho\sin\theta$

Then, $\rho = \sqrt{u_x^2 + u_y^2}$ and $\theta = \arctan\frac{u_x}{u_y}$

where the ρ axis corresponds to frequency and has a range of 0 to $\frac{1}{2}$ length of an side. θ describes the direction of frequency and has a range of 0° to 360°.

Therefore, rotation can be recovered first, regardless the translation parameters. Using a polar DFT, the rotation over the angle θ is reduced to a shift over θ, which can be robustly recovered using the phase-correlation procedure (11). Using (13) to estimate the rotation angle θ results in an ambiguity by a factor of π [29] in the estimation of the rotation angle (note the π ambiguity is due to the conjugate symmetry of the Fourier transform of image). This ambiguity can be resolved by applying both hypotheses θ and $\theta+\pi$ and recover the translational motion (d_x, d_y) and the correlation peak of each hypothesis. The rotation hypothesis and translation values, which are related to the highest correlation peak, are chosen as the result.

5.2 Matching under sub-pixel shift

We propose in this sub-section the sub-pixel accuracy based on the auto- and cross-bispectrum for obtaining high accuracy sub-pixel motion estimates.

A shift of the image parallel to the image plane can be expressed in Fourier domain as a linear phase shift:

$$\begin{aligned} G(u_x, u_y) &= \int_{-\infty}^{+\infty}\int_{-\infty}^{+\infty} f(x + d_x, y + d_y)e^{-i2\pi(u_x d_x + u_y d_y)}dxdy \\ &= e^{-i2\pi(u_x d_x + u_y d_y)}F(u_x, u_y) \end{aligned} \tag{14}$$

Using the relation (14) we can transform (10) as:

$$B^{gfg}(u_x, u_y) = B^{fff}(u_x, u_y)e^{-i2\pi(u_x d_x + u_y d_y)} \tag{15}$$

The correlation surface between $g(x, y)$ and $f(x, y)$ is defined as [23]:

$$S(r_x, r_y) = \mathcal{F}^{-2}[\frac{B^{gfg}(u_x, u_y)}{|B^{fff}(u_x, u_y)|}] = \delta(x - d_x, y - d_y) \tag{16}$$

Motivated by searching for a method which represents advantages of the auto-bispectrum described above, we will investigate, here, the possibility of extracting sub-pixel shifts between two fingerprint images. For this purpose, we will derive analytic expressions to extend the shift model to sub-pixel shift estimation.
In (16) the coordinates (rm_x, rm_y) of the maximum of the real valued array $S(r)$ can be used as an estimate of the horizontal and vertical components of motion between $g(x, y)$ and $f(x, y)$ as follows:

$$(rm_x, rm_y) = \arg\max(S(r_x, r_y)) \tag{17}$$

Sub-pixel accuracy of motion measurements is obtained by variable separable fitting performed in the neighborhood of the maximum using 1-D parabolic-fit interpolation method. In our application, the parabolic fitting is performed near the peak and only requires a few operations.
The parabola has the form: $S(rm_x) = arm_x^2 + brm_x + c$.
Using the notation in (17) above, prototype function are fitted to the triplets [32]:

$$[S(rm_x - 1), S(rm_x), S(rm_x + 1)], \tag{18}$$

and

$$[S(rm_y - 1), S(rm_y), S(rm_y + 1)]. \tag{19}$$

i.e. the maximum peak of the surface and its two neighboring values on either side, vertically and horizontally. The location of the maximum of the fitted function provides the required sub-pixel motion estimate $\hat{d} = (\hat{d}_x, \hat{d}_y)$. The fitting a parabolic function horizontally to the data triplet (18) yields a closed-from solution for the horizontal component of the motion estimate $\hat{d}_x$ as follows [32]:

$$\hat{d}_x = -\frac{b}{2a} = \frac{S(rm_x - 1) - S(rm_x + 1)}{2[S(rm_x + 1) - 2S(rm_x) + S(rm_x - 1)]}. \tag{20}$$

The fractional part $\hat{d}_y$ of the vertical component can be obtained in a similar way using (19) instead of (18).
Finally the horizontal and vertical components of the sub-pixel accurate motion estimate are obtained by computing the location of the maxima of each of the above fitted quadratics.

6 Experimental results

This section reports some experimental results obtained by proposed method and compares it with other approaches, using three fingerprint databases commonly adopted by the scientific community, namely, FVC2002 DB1 database [33], FVC2004 DB3 database [34] and FVC2006 DB2 database [35]. While both the FVC2002 DB1 and FVC2004 DB3 databases contain 100 different fingers with 8 impressions (samples) per finger resulting in 800 images, the FVC2006 DB2 database consists of 140 fingers with 12 impressions per finger in depth (total 1680 fingerprint). In the following, we denote with DSP-PS the method introduced here, with POACB-based approach proposed in our previous work [37] and with POC-based approach described in [9].
The matching performance of a fingerprint recognition method is evaluated by means of several measures. The most commonly used are the false acceptance rate (FAR), the false rejection rate (FRR), and the equal error rate (EER). FAR is the probability that the method gives a "match" decision for fingerprints that are not from the same finger. FRR is the probability that the method gives a "non-match" decision for fingerprints that are from the same finger. For each algorithm and for each database, EER and receiver operating characteristics (ROC)

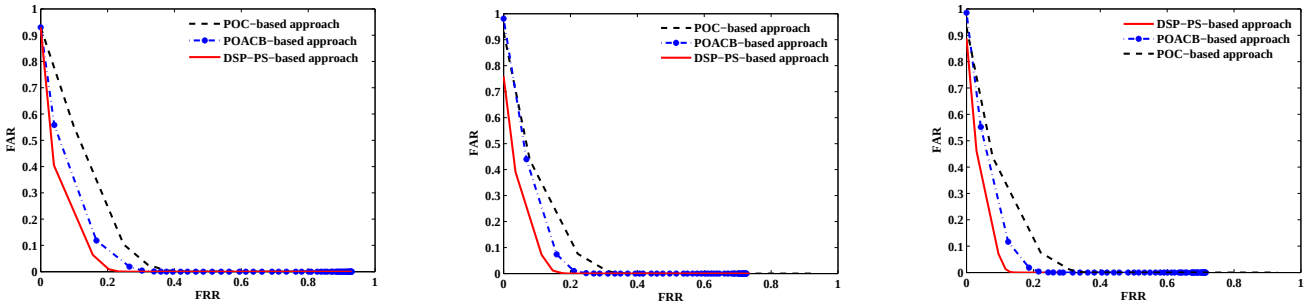

Figure 1: ROC curves for the three approaches: (a) FVC2002 DB1 database, (b) FVC2004 DB3 database and (c) FVC2006 DB2 database.

Methods \ Database	FVC2002 DB1		FVC2004 DB3		FVC2006 DB2	
	ERR	FRR at FAR=0%	ERR	FRR at FAR=0%	ERR	FRR at FAR=0%
POC	0.16	38%	0.15	31%	0.19	33%
POACB	0.14	30%	0.13	23%	0.14	21%
DSP-PS	0.10	21%	0.11	16%	0.09	13%

Table 1: Comparison of the EER and FRR at FAR=0% for the three methods

curve are used as performance indicators. The ROC(t) curve is a plot between FAR and FRR for different values of the threshold, t. Given two algorithms and their ROC curves, the better algorithm is one whose ROC curve is lower than other's ROC curve over a suitably large range of threshold values t. The EER is the rate at which the FAR is equal to the FRR. The lower the EER, the better is the method. For each algorithm the impostor and genuine score distributions are also reported.

The performance of the algorithms is evaluated by the ROC curve. The ROC curves for the different algorithms on the three databases mentioned above are shown in Figure 1. It can be seen that the FRR of the three methods are comparable at higher FAR values. At lower values of FAR, our proposed method clearly shows as good performance as that of POACB-based algorithm and both are superior to the POC-based algorithm. However, DSP-PS exhibits significantly higher performance, since its ROC curve is located at lower FRR/FAR region than those of the POACB-based and the POC-based algorithms. From the graphs it is evident that the proposed fingerprint recognition performs better than other approaches on all the three databases.

Table 1 highlights some relevant points on the ROC curves: it is well evident that the proposed method exhibits a markedly higher accuracy at any FAR. Note the total number of genuine tests is 2800, 2800 and 9240 for FVC2002 DB1, FVC2004 DB3 and FVC2006 DB2 database respectively. The total number of false acceptance tests is 4950, 4950 and 9730 for the FVC2002 DB1, FVC2004 DB3 and FVC2006 DB2 database respectively. The proposed method clearly outperforms other methods. It achieves an EER of less than 1% on all the three databases. As is observed in the above experiments, the proposed algorithm is particularly useful for verifying difficult fingerprint images.

The most remarkable property of DSP-PS-based approach compared to other methods is its accuracy in fingerprint matching. Figures 2 and 3 show examples of genuine matching and impostor matching using three algorithms. It can be seen that the DSP-PS and POACB methods are comparable in the case of genune matching, and both are provide the higher correlation peak and better discrimination capability than that of the POC-based approach. The height of the peak can be used as a good similarity measure for fingerprint matching. If we consider correlation output for an imposter matching, the POC-based algorithm gives a peak that may cause a matching error. However, DSP-PS and POACB approaches don't have any peak as shown in Figures

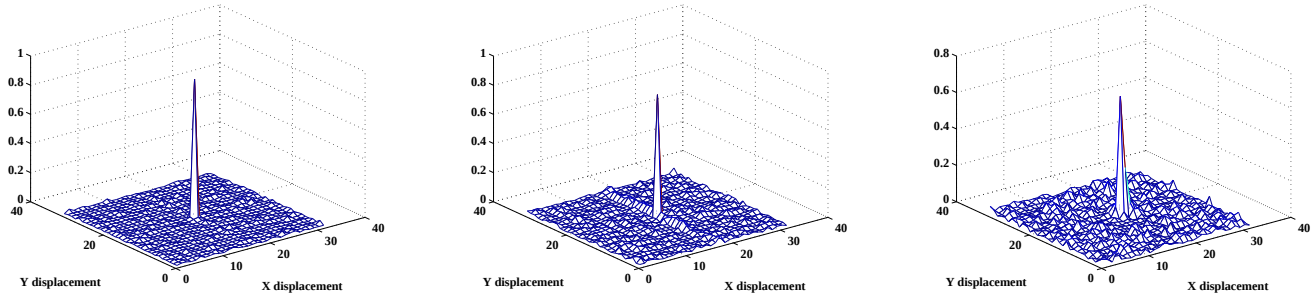

(a) (b) (c)

Figure 2: Example of genuine matching: (a) DSP-PS-based approach, (b) POACB-based approach and (c) POC-based approach.

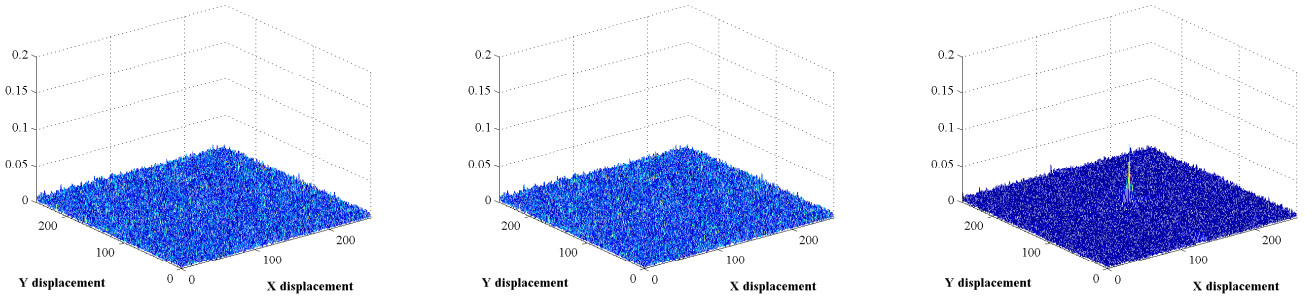

(a) (b) (c)

Figure 3: Example of impostor matching: (a) DSP-PS-based approach, (b) POACB-based approach and (c) POC-based approach.

3(a) and 3(b). Because, the auto-bispectrum retains both amplitude and phase information from the FT of a signal, unlike the POC-based algorithm. The phase of the FT contains important shape information. Therefore, the DSP-PS and POACB algorithms minimize the influence of the noise and simplifie the identification of the dominant peak on the correlation output.

In order to test the algorithm's robustness to translation and rotation, we selected sixty registered fingerprints from the FVC2006 DB2 database. First, these sixty images are translated to the left and rotated. The matching result is shown in Table 2. Each input fingerprint image is compared with the all fingerprints step by step, and correlation between two fingerprint images is found out. The input fingerprint image that gives the highest correlation peak is selected as the shift-rotation-normalized image. From the Table 2, we can observe that even after a rotation of 10° and 15% translation to the left, recognition accuracy is more than 94,73%. In other words, most useful information does not get lost due to small translation and rotation. This proves that the DSP-PS-based approach is reliable and robust to small translation and rotation. It is very clear that the more the image is translated and rotated, the more information will get lost and the poorer the matching results will be. The correct matching result for shifted-rotated images can prove that our approach works also for right, up and down translation.

7 Conclusion

In this paper, an effective scheme in the third-order frequency domain for fingerprint images by learning from the images has been proposed. Our scheme based on HOS features that are invariant to translation and rotation is shown to accurately distinguish between similar (or dissimilar) fingerprint patterns. The proposed technique

Translation	Rotation angle	Accuracy		
		DSP-PS	POACB	POC
10%	5°	98.26%	98.03%	96.23%
15%	10°	94,73%	93,07%	88,71%
25%	20°	80.12%	81.35%	76.91%
50%	40°	37,45%	35,75%	31,20%

Table 2: Algorithm's performance in presence of translation and rotation.

was compared to some other frequency domain methods in simulations and practical experiments. Both proved the validity and high precision of our algorithm. The obtained results are considerably promising since very low FAR, FRR and high accuracy.

References

[1] Maltoni, D., Maio, D., Jain, A.K., Prabhakar, S, "Handbook of Fingerprint Recognition", 2nd edn. Springer, New York. 2009.

[2] Jain, A. K. ; Feng, J. & Nandakumar, K, "Fingerprint Matching, Computer", Vol. 43, No. 2, pp. 36-44. 2010.

[3] C. D. Kuglin and D. C. Hines,"The phase correlation image alignment method", in Proceedings International Conference on Cybernetics and Society IEEE, pp. 163- 165. 1975.

[4] K. Takita, T. Aoki, Y. Sasaki, T. Higuchi, and K. Kobayashi," High-accuracy subpixel image registration based on phase-only correlation", IEICE Trans. Fundam. Electron. Commun. Comput. Sci.E86-A , 1925-1934. 2003.

[5] A. M. Bazen, G. T. B. Verwaaijen, S. H. Gerez, L. P. J. Veelenturf, and B. J. v. d. Zwaag, "A correlation-based fingerprint verification system", in ProRISC Workshop on Circuits, Systems and Signal Processing, Veldhoven, the Netherlands, pp. 205-213. 2000.

[6] A. Jain, A. Ross, and S. Prabhakar,"Fingerprint matching using minutiae and texture features", in International Conference on Image Processing, vol. 3, pp. 282-285 vol.3. 2001.

[7] K. Nandakumar and A. K. Jain, "Local correlation-based fingerprint matching", in Indian Conference on Computer Vision, Graphics and Image Processing (ICVGIP), Kolkata, India, pp. 503-508. 2004.

[8] K. Ito, A. Morita, T. Aoki, T. Higuchi, H. Nakajima, and K. Kobayashi, "A Fingerprint Recognition Algorithm using Phase-based Image Matching for Low Quality Finger prints", Proceedings of IEEE International Conference on Image Processing, Genoa, Italy, vol. 2, pp. 33-36, September, 2005.

[9] K. Ito, H. Nakajima, K. Kobayashi, T. Aoki, and T. Higuchi, "A fingerprint matching algorithm using phase-only correlation", IEICE Trans. Fundamentals, Vol. E87-A(3):pages 682-691, March 2004.

[10] Ouyang, Z., Feng, J., Su, F., Cai, A, "Fingerprint Matching with Rotation-Descriptor Texture Features", In: Proc. 18th Int'l Conf. on Pattern Recognition (ICPR'06), vol. 4, pp. 417-420. 2006.

[11] J. Zhang, Z. Ou and H. Wei, "Fingerprint Matching using Phase only Correlation and Fourier-Mellin Transforms", Proceedings of the 6th International Conference on Intelligent Systems Design and Applications, Jian, China, pp. 379-383, 2006.

[12] A. Cavusoglu and S. Gorgunoglu, "A Robust Correlation based Fingerprint Matching Algorithm for Verification", Journal of Applied Sciences, vol. 7, no. 21, pp. 3286-3291, 2007.

[13] He, Z., Zhao, X., Zhang, S,"Low-quality fingerprint recognition using a limited ellipse-band-based matching method", JOSA A, 32, (6), pp. 1171-1179. 2015.

[14] P. Elena and B. Pavol, "Industrial production surety factor increasing by a system of fingerprint verification", in International Conference on Information Science, Electronics and Electrical Engineering (ISEEE) , pp. 493- 497. 2014.

[15] T. Amornraksa and S. Tachaphetpiboon, "Fingerprint recognition using DCT features", Electron. Lett. 42 , 522-523. 2006.

[16] Yang, J., Xiong, N., Vasilakos, A.V, "Two-stage enhancement scheme for low-quality fingerprint images by learning from the images", IEEE Trans. Human–Machine Syst.,43, (2), pp. 235-248. 2013.

[17] Sheng, W. ; Howells, G. ; Fairhurst, M. & Deravi, F, "A Memetic Fingerprint Matching Algorithm", IEEE Transactions on Information Forensics and Security, Vol. 2, No. 3, pp. 402-412. 2007.

[18] Cappelli, R. ; Ferrara, M. & Maltoni, D, "Minutia Cylinder-Code.: A New Representation and Matching Technique for Fingerprint Recognition", IEEE Trans on Pattern Analysis and Machine Intelligence, Vol. 32, No. 12, pp. 2128-2141. 2010.

[19] Xu, H. ; Veldhuis, R. N. J. ; Bazen, A. M. ; Kevenaar, T. A. M. ; Akkermans, T. A. H. M. & Gokberk, B, "Fingerprint Verification Using Spectral Minutiae Representations", IEEE Transactions on Information Forensics and Security, Vol. 4, No.3, pp. 397-409. 2009.

[20] Xu, H. ; Veldhuis, R. N. J. ; Kevenaar, T. A. M. & Akkermans, T. A. H. M, " A Fast Minutiae-Based Fingerprint Recognition System", IEEE Systems Journal, Vol. 3, No. 4, pp. 418-427. 2009.

[21] Takeuchi, H. ; Umezaki, T. ; Matsumoto, N. & Hirabayashi, K, "Evaluation of Low-Quality Images and Imaging Enhancement Methods for Fingerprint Verification", Electronics and Communications in Japan, Part 3, Vol. 90, No. 10, pp. 40-53. 2007.

[22] Hashad, F. G. ; Halim, T. M. ; Diab, S. M. ; Sallam, B. M. & Abd ElSamie, F. E, "Fingerprint Recognition Using Mel-Frequency Cepstral Coefficients, Pattern Recognition and Image Analysis", Vol. 20, No. 3, pp. 360-369. 2010.

[23] E. M. Ismaili Alaoui and E. Ibn-Elhaj, "A robust hierarchical motion estimation algorithm in noisy image sequences in the bispectrum domain", In SIVP. Springer-Verlag London, 2008.

[24] Nikias, C.L., Petropulu, A.P, "Higher-Order Spectra Analysis: A Nonlinear Signal Processing Framework", Prentice-Hall, Englewood Cliffs. 1993.

[25] Sadler, B.M., Giannakis, G.B, "Image sequence analysis and reconstruction from the bispectrum", In: Proceedings of Conference on Information Sciences and Systems, p. 242. Johns Hopkins University, Baltimore. 1989.

[26] V. Chandran, B. Carswell, B. Boashash, S. Elgar, "Pattern recognition using invariants defined from higher order spectra :2-D image inputs". IEEE Trans on Image Processing, 6(5), pp. 703-712. 1997.

[27] Q.S. Chen, M. Defrise, and F. Deconinck;"Symmetric phase-only matched filtering of Fourier-Mellin transforms for image registration and recognition", IEEE Transactions on Pattern Analysis and Machine Intelligence, vol. 16, no. 12, pp. 1156-1168, 1994.

[28] Gardenier, P.H., McCallum, B.C. and Bates, R.H.T, "Fourier transform magnitudes are unique pattern recognition templates", Biological Cybernetics, Vol. 54, Pp. 385-391. 1986.

[29] S. Reddy and B. N. Chatterji, "An FFT-based technique for translation, rotation, and scale-invariant image registration",IEEE Trans. on Image Processing, 3(8):1266-1270, August 1996.

[30] Alshebeili, S.; Cetin, A. E, "A phase reconstruction algorithm from bispectrum (seismic reflection data)", IEEE Transactions on Geoscience and Remote Sensing, vol. 28, issue 2, pp. 166-170. DOI 10.1109/36.46695 . 1990.

[31] Bates, R.H.T, "Aspects of the Erlangen-bispectrum", Optik, Vol. 76, No.1, Pp. 23-26. 1987.

[32] E. M. Ismaili Alaoui, E. Ibn-Elhaj, and E. H. Bouyakhf, "A robust subpixel motion estimation algorithm using hos in the parametric domain", In EURASIP Journal on Image and Video Proc, No 3, 2009.

[33] Proc. Second Int'l Competition for Fingerprint Verification Algorithms (FVC 2002), http://bias.csr.unibo.it/fvc2002, 2002.

[34] FVC2004-Third International Fingerprint Verification Competition. http: //bias.csr.unibo.it/fvc2004, 2004.

[35] Fourth International Fingerprint Verification Competition. http://bias.csr. unibo.it/fvc2006.

[36] E. M. Ismaili Alaoui, E. Ibn-Elhaj, and E. H. Bouyakhf, "Noise-insensitive image optimal flow estimation using higher-order statistics",In J. Opt. Soc. Am. A, Vol 26, No.5, Dec 2009.

[37] E. M. Ismaili Alaoui, E. Ibn-Elhaj, "A new method for fingerprint matching using phase-only auto- and cross-bispectrum",In Signal, Image and Video Processing. Springer-Verlag London. July 2016.